Continental Shelf Research 122 (2016) 14–28

Contents lists available at ScienceDirect

Continental Shelf Research

journal homepage: www.elsevier.com/locate/csr

Research papers

A numerical investigation of the interannual-to-interpentadal variability of the along-shelf transport in the Middle Atlantic Bight

Shuwen Zhang [a,*], Yiyong Luo [b], Lewis M. Rothstein [a], Kun Gao [a]

[a] Graduate School of Oceanography, University of Rhode Island, 215 South Ferry Road, Narragansett, RI 02882, USA
[b] Physical Oceanography Laboratory, Ocean University of China, 238 Songling Road, Qingdao, Shandong, 266100, China

ARTICLE INFO

Article history:
Received 25 August 2015
Received in revised form
19 December 2015
Accepted 21 March 2016
Available online 25 March 2016

Keywords:
Interannual variability
Along-shelf transport
Middle Atlantic Bight

ABSTRACT

A numerical simulation using the Regional Ocean Modeling System (ROMS) indicates that there was significant interannual-to-interpentadal variability of along-shelf transport and water properties over the Middle Atlantic Bight (MAB) from 2004 to 2013. To examine the relative contribution from local atmospheric forcing versus remote oceanic open boundary forcing to such low-frequency variability, we implement a suite of process oriented numerical experiments. Results show that the interannual variability is dominated by remote forcing from the open boundaries of the region rather than by local atmospheric forcing. The penetration of the Labrador Current into the region contributes to a significant increase of along-shelf transport in the winters of 2009 and 2010. By contrast, the anti-cyclonic mesoscale eddies associated with the Gulf Stream decrease the background along-shelf jet and, in certain cases, even reverse the along-shelf transport. In addition, the along-shelf transport appears to possess an interpentadal variation, i.e., weaker during 2004–2008 but stronger during 2009–2013, which is found caused by the migration of the Gulf Stream.

1. Introduction

The Northeast U.S. continental shelf/slope region encompasses an area of approximately 260,000 km^2 from the Scotia Shelf in the north to Cape Hatteras in the south, covering the Gulf of Maine/Georges Bank (GoM/GB) and the entire Middle Atlantic Bight (MAB). The MAB shelf is widest off southern New England, extending over 200 km seaward from shore, and is relatively narrower off Cape Hatteras, where the shelfbreak is approximately 30 km from shore (Fig. 1). The hydrography in the MAB region is featured with cooler and fresher shelf water separated from warmer and saltier slope water by a shelfbreak front (Mountain, 2003). Associated with this front is a narrow, southwestward flowing baroclinic jet that, which to leading order is in geostrophic balance.

Quantifying the along-shelf transports and cross-shelf exchanges of the shelfbreak region has been a long-standing research topic. A mass and salinity balance in the MAB indicates that approximately three quarters of the water that passes south of Nantucket leaves the shelf by the time it reaches Delaware and a third of the water that is lost is replaced by the more saline waters of the upper slope (Biscaye et al., 1994). Clearly, these transport changes must involve a considerable amount of cross-shelf exchanges of mass, heat, freshwater, and nutrients. Intensive in-situ studies since the 1970s have been carried out using moorings and hydrographic surveys at various locations during different time periods (NESDE, Beardsley and Flagg, 1976; NSFE, Beardsley et al., 1985; SEEP-I, Walsh et al., 1988; SEEP-II, Biscaye et al., 1994; and CMO/PRIMER, Dickey and Williams, 2001), all with the common goal of understanding the dynamics of the front and the critical shelf and slope exchange processes. The hydrography of the shelfbreak region has been described in a number of syntheses, the latest of which is produced by Linder and Gawarkiewicz (1998) and Linder et al. (2006).

High spatial resolution and temporally continuous numerical simulations have become important tools for obtaining a better understanding of the MAB shelf/slope circulation and for quantifying its variations. Chen and He (2010) performed a high-resolution hindcast simulation with a focus on the mean state of shelfbreak circulation and the total water transport across 200 m isobath over the MAB during years of 2004–2008. However, their 4-year simulations are insufficient for addressing the interannual variability of the shelfbreak front/jet system that might occur in response to local forcing and/or basin-scale natural climate variability. Xu and Oey (2011) conducted numerical experiments with realistic forcing to study the physical mechanisms contributing to the mean, seasonal, and interannual variability of the

* Corresponding author.
E-mail addresses: shuwen_zhang@my.uri.edu (S. Zhang), yiyongluo@ouc.edu.cn (Y. Luo), lrothstein@gso.uri.edu (L.M. Rothstein), kun_gao@uri.edu (K. Gao).

http://dx.doi.org/10.1016/j.csr.2016.03.022
0278-4343/

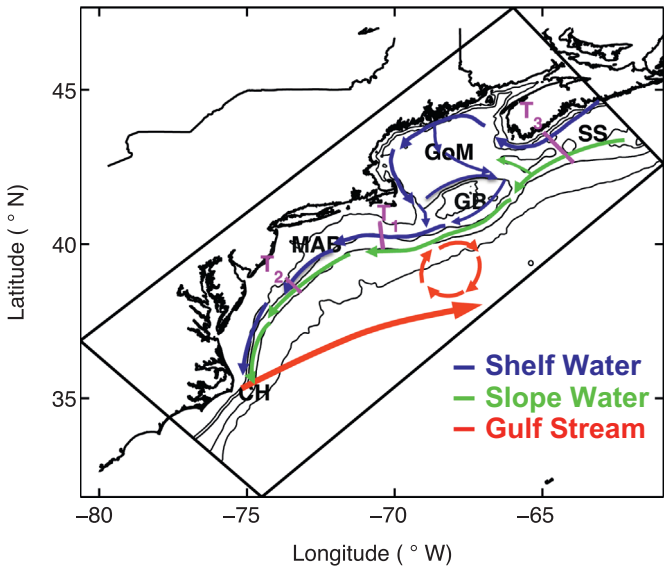

Fig. 1. Map of the Northeast U.S. continental shelf/slope region and the regional-scale ROMS model domain (black box). The primary geographical features are the Scotia Shelf (SS), the Gulf of Maine (GoM), Georges Bank (GB), the Middle Atlantic Bight (MAB) and Cape Hatteras (CH). The 50, 100, 1000 and 3000 m isobaths are represented by black contours. Principal circulation features are equatorward flow of shelf and slope waters and poleward flow of the Gulf Stream; a warm core ring is also depicted (Based on http://www.nefsc.noaa.gov/ecosys/ecology/Oceanography/). The three selected cross-shelf sections for analyses are marked as T_1, T_2 and T_3.

along-shelf pressure gradient in the MAB, which is the driving force for the MAB current system. But their model specified steady transports across open boundaries, so the impact of the basin-scale variability is neglected.

The interannual variations in the Northeast U.S. continental shelf/slope region are very likely linked to processes on a much larger scale, since the entire area is located within a western boundary 'confluence zone', with the subpolar gyre and Labrador Current moving southwestward, and the subtropical gyre and the Gulf Stream moving northeastward (Beardsley and Flagg, 1976). The variability of the Labrador Current and the Gulf Stream, as well as the sea level rise along the mid-Atlantic coastal region are all associated with the variability of the Atlantic Meridional Overturning Circulation (AMOC), which is under the impact of large-scale variations in the atmospheric pressure and wind patterns over the North Atlantic, characterized by the North Atlantic Oscillation (NAO) index (McCarthy et al., 2012; Smeed et al., 2014; Ezer et al., 2013, Ezer, 2015). For instance, the large drop of the NAO index in 1996 was reported responsible for the cold/fresh Labrador Slope Water flux into the Gulf of Maine through the Northeast Channel in 1998 (Drinkwater et al., 2002; Pershing et al., 2001; Greene and Pershing, 2003). There are studies suggesting that the interannual to decadal variations of the sea level along the mid-Atlantic coast are significantly influenced by the variations of the Gulf Stream (Ezer et al., 2013) and the AMOC (Ezer, 2015). And the slope current transport in MAB region can be affected by the position and strength of Gulf Stream through the change of the sea levels near the coast (Ezer et al., 2013; Ezer, 2015). Luo et al. (2013) investigated the correlation between the along-shelf transport off southern New England and the NAO index, and suggested that the along-shelf transport is negatively correlated with the NAO index with a lag of 13 months. However, their 6-year simulation (2004–2009) does not yield a compelling statistical argument.

In this study, we aim to understand the interannual variability of along-shelf transport in the MAB region and the underlying physical mechanisms controlling such variability by extending the model simulation performed by Luo et al. (2013). Specifically, we extend the regional model domain in Luo et al. (2013) to include the influence of the Gulf Stream, and increase the length of the simulation to 10 years (2004–2013). The rest of the paper is organized as follows. The numerical model configuration, a realistic simulation and a suite of process-oriented numerical experiments are described in Section 2, followed by model verification in Section 3. The mean state of the shelf/slope circulation system during the decade under investigation is discussed in Section 4. Analyses of the interannual variability of the along-shelf transport and its origins are presented in Section 5, and the underlying physical mechanisms are presented in Section 6. The variation of the along-shelf transport of the two pentads during the 10-year simulation and the plausible mechanism are explored in Section 7. Finally, Section 8 summarizes the important findings of this study.

2. Experiment design

2.1. Realistic forcing simulation

Our numerical simulations are based on the Regional Ocean Modeling System (ROMS), which is a free-surface, hydrostatic, terrain-following, primitive equations ocean model widely used by the scientific communities for estuarine, coastal and basin-scale ocean applications. The algorithms that comprise ROMS computational nonlinear kernel are described in detail in Shchepetkin and McWilliams (2005). Our regional model domain is bounded by Cape Hatteras to the south and the Scotia Shelf to the north, covering the GoM/GB and the entire MAB (black box in Fig. 1), with a constant 5 km horizontal resolution. Compared with the model domain applied by Luo et al. (2013), the model domain in this study is extended further south in order to resolve part of the Gulf Stream. Clearly such a small model domain is still not ideal for resolving the Gulf Stream. However, we find that the model can capture the mean structure and the transport of the Gulf Stream off Cape Hatteras (10-year average value of 75 Sv) reasonably well as compared with previous studies (Knauss, 1969; Halkin and Rossby, 1985). The topography is derived from the 1 arc-minute ETOPO1 Global Relief Model of Earth's surface and the bathymetry ranges from 10 to 5000 m within our model domain. There are 30 terrain-following levels in the water column with the highest resolution of 0.33 m near surface and the lowest resolution of 485.3 m at depth.

The open boundary forcing is provided by a global eddy-resolving numerical solution produced by the Hybrid Coordinate Ocean Model with the Navy Coupled Ocean Data Assimilation scheme (HYCOM/NCODA, http://hycom.org/dataserver/glb-analysis). HYCOM/NCODA provides three-dimensional ocean state variables with 1/12° resolution in both longitude and latitude, with 32 vertical layers. The output used for this study spans from January 2004 to December 2013; a monthly climatology for each variable (velocity, temperature and salinity) is used as the boundary forcing for the model spin-up.

Free surface and depth-averaged velocities are specified using the method of Flather (1976) with external sub-tidal values taken from HYCOM/NCODA plus five tidal constituents (M_2, N_2, S_2, O_1, K_1) from the global ocean tides model TPXO7.2 (http://volkov.oce.orst.edu/tides/TPXO7.2.html). The model has been found capable of producing a realistic simulation of tidal magnitude and tidal currents (Luo et al., 2013). The tidal forcing introduces tide-induced mixing in the model, hypothesized as an important element of the regional circulation. In addition, a quadratic drag formulation is employed for bottom stress, and the Mellor-Yamada Level 2.5 turbulence closure scheme is chosen for the vertical mixing parameterization (Mellor and Yamada, 1982).

The local surface forcing is derived from the National Oceanic and Atmospheric Administration (NOAA) National Centers for Environmental Prediction North America Regional Reanalysis (NCEP/NARR), which has spatial and temporal resolutions of 32 km and 3 hours, respectively. All of the atmospheric components (winds, air temperature, air pressure, relative humidity, rainfall rate, short and long wave radiations) are averaged into daily intervals, spanning from January 01, 2004 to December 31, 2013. Bulk formulae are used for the computation of the surface momentum, sensible and latent heat fluxes. To further constrain the spatial pattern of the net surface heat flux, a thermal relaxation term is implemented following He and Weisberg (2002):

$$K_H \frac{\partial T}{\partial Z} = \frac{Q}{\rho C_p} + c\left(T_{obs} - T_{mod}\right)$$

where K_H is a vertical diffusivity coefficient, Q is the net heat flux, and ρ and C_p are the seawater density and specific heat capacity, respectively. The relaxation coefficient c is set as 0.8 m day^{-1}, and the model simulated sea surface temperature T_{mod} is subtracted from T_{obs}, which is the daily blended cloud-free sea surface temperature obtained from the Jet Propulsion Laboratory Multi-scale Ultra-high Resolution Sea Surface Temperature (JPL MUR-SST, http://mur.jpl.nasa.gov/).

Fresh water outflow used in the model is based on the United States Geological Survey (USGS, http://www.usgs.gov/water/) stream gauge climatological datasets. Seventeen major rivers are considered, including, from north to south, St. Johns River, St. Croix River, Penobscot River, Kennebec River, Androscoggin River, Merrimac River, Neponset River, runoff from Narragansett Bay (including Taunton River, Blackstone River, Pawtuxet River), Pawcatuck River, Connecticut River, Housatonic River, Hudson River, Delaware River and Potomac River.

The model is initialized with January climatological condition, and the barotropic and baroclinic time steps are set to 2.5 and 75 seconds, respectively. The model is first spun up with monthly climatological forcing for 2 years, and then integrated with the realistic surface and open boundary forcing from January 2004 to December 2013 to produce the targeted 10-year dataset. We label this experiment as REAL in Table 1.

2.2. Experimental hierarchy

In addition to the above-described REAL experiment, we also perform five parallel experiments to examine the response of the along-shelf front/jet system to various external forcing, including local atmospheric forcing and remote forcing from both upstream and offshore open boundaries (Table 1). For all of the additional experiments, the configurations of the 2-year spin-up run are the same as REAL. Below we describe the difference between each additional experiment and REAL in the 10-year simulation (2004–2013). Experiment WIND investigates the influence of the surface winds; so the monthly climatological wind fields are used. Experiment SURF aims to examine the combined impacts of surface momentum and buoyancy fluxes, and therefore all of the atmospheric components and the SST fields used in the thermal relaxation are replaced with their monthly climatology. Experiment OBCs is designed to test the effects of the open boundary forcing, and therefore the monthly climatological forcing at all three open boundaries is applied. The final two experiments are designed to further investigate the impacts of upstream and offshore forcing, respectively. Experiment UPSTREAM uses monthly climatological forcing at the upstream open boundary (i.e., the northern open boundary, where the southwestward Labrador Current flow into the region), while experiment OFFSHORE applies monthly climatological forcing at the offshore open boundaries (i.e., the eastern and southern boundaries, where the subtropical gyre and the Gulf Stream interact with this region).

Table 1
A summary of the numerical experiments conducted in this study.

Experiment name	Surface forcing		Remote forcing	
	Wind	Buoyancy	Upstream	Offshore
REAL	Daily 10 Yr		Monthly 10 Yr	
WIND	Climatology	Daily 10 Yr	Monthly 10 Yr	
SURF	Climatology		Monthly 10 Yr	
OBCs	Daily 10 Yr		Climatology	
UPSTREAM	Daily 10 Yr		Climatology	Monthly 10 Yr
OFFSHORE	Daily 10 Yr		Monthly 10 Yr	Climatology

3. Model validation

In this section, we compare the model results from experiment REAL with available observations to validate that the model demonstrates reasonable skill in capturing the essential features of the MAB shelf and slope circulation and water properties. A direct comparison of depth-averaged currents at 27 locations over the MAB between the model and the observations is presented in Fig. 2. The observations are from Lentz (2008a) in which he obtained the depth-averaged currents by analyzing current time series longer than 200 days. The model results are derived by averaging the currents during 2004–2013 from experiment REAL. Consistent with the observations, the model shows that the depth-average currents at all sites are approximately along isobaths and increase with water depth over the shelf from ~3 cm s^{-1} on the inner shelf to more than 10 cm s^{-1} in 100 m water depth. While differences in both speed and direction exist for each pair of comparisons, the model overall does a satisfying job, with the RMSEs of the speed and the direction being less than 1 cm s^{-1} and 10°, respectively. These differences could be attributed to the model resolution and topographic smoothing, especially for one

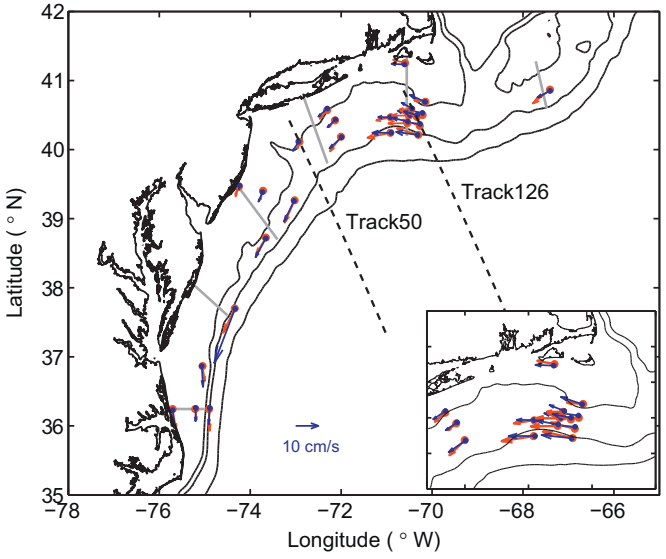

Fig. 2. Comparison of depth-averaged currents between the model (blue arrows) and observations (red arrows); the southern New England shelf area is zoomed in and inserted in the lower right corner. Thick light-grey lines indicate six cross-shelf transects from coast to shelfbreak; their corresponding locations are listed in Table 2. Black dashed lines are the two satellite tracks, along which the SSHA data are sampled. The 50, 100, and 1000 m isobaths are also shown. (For interpretation of the references to color in this figure legend, the reader is referred to the web version of this article.)

Table 2
Comparison between modeled and observed (Lentz, 2008a) along-shelf volume transport at six cross-shelf transects within the MAB. The standard deviations are listed in parenthesis. The coastal endpoints of each transect and the water depths at the shelfbreak are also listed.

Transect	Lat (°N)	Lon (°W)	Shelfbreak depth (m)	Transport (Sv)	
				Observation	Model
Georges Bank	41.28°	67.72°	95	0.44	0.43 ($\pm$0.10)
Cape Cod	41.33°	70.56°	125	0.64	0.66 ($\pm$0.13)
Long Island	40.75°	72.82°	90	0.41	0.44 ($\pm$0.10)
New Jersey	39.46°	74.26°	85	0.27	0.23 ($\pm$0.06)
Maryland	38.03°	75.22°	75	0.16	0.18 ($\pm$0.05)
North Carolina	36.25°	75.71°	45	0.09	0.09 ($\pm$0.02)

site off the Maryland coast. Next, the model simulated along-shelf volume transport is compared at six cross-shelf transects (thick light-grey lines in Fig. 2) with those reported by Lentz (2008a) (Table 2). There is good agreement between the modeled and observed transports. Overall, the along-shelf transport decreases from Cape Cod to North Carolina, consistent with the previous finding by Lozier and Gawarkiewicz (2001) that the shelf water is continually entrained into the offshore shelfbreak frontal jet from north to south over the MAB.

We next compare the modeled climatological temperature and salinity fields at mid-depth (40–55 m) over the MAB and the Georges Bank region with the climatology constructed by Linder and Gawarkiewicz (1998) and Linder et al. (2006) based on observations. This comparison (Fig. 3a, b) is presented in four seasons: winter (Jan-Feb-Mar), spring (Apr-May-Jun), summer (Jul-Aug-Sep), and fall (Oct-Nov-Dec). The model generally captures the observed thermohaline features well. There is a large seasonal variation in the cross-shelf thermal gradient with the largest value near the 100 m isobath (black contours in Fig. 3a), corresponding to the position of the shelfbreak front. In winter, the shelf water temperatures increase offshore by virtue of surface cooling throughout the region. Surface heating starts to warm shelf water during the spring and leads to the development of a shallow seasonal thermocline over the mid-depth. During summer, cross-shelf thermal gradients are found in two regions with cold water located on the shelf. One is located to the southeast of Georges Bank, resulting from the intensified anti-cyclonic circulation around the bank transporting relatively cold, fresh water from the western Gulf of Maine and across the Northeast Channel. The other region spreads from the southern New England shelf over the Delaware/Maryland shelf, and is the residual cold winter water that remains under the shallow seasonal thermocline, the so-called 'cold pool', that persists from May through October (Houghton et al., 1982; Lentz, 2008b). In contrast to the temperature, seasonal variations in both salinity (Manning, 1991; Mountain, 2003) and cross-shelf salinity gradient (Shearman and Lentz, 2003) tend to be small, except over the inner shelf (depth $<$ 60 m) where there can be an enhanced cross-shelf salinity gradient due to spring runoff (Ullman and Codiga, 2004). The plan view maps (Fig. 3b) clearly show the proximity of the 34.5 isohaline, which defines the core of the shelfbreak front at mid-depth to the bathymetry offshore of the 100 m isobath throughout the MAB.

Finally, we examine the model skill in reproducing the interannual variability of the sea surface height by comparing model simulations with satellite altimeter data. We obtained the 1/3° $\times$ 1/3° along-track sea surface height anomaly (SSHA) from the AVISO (Archiving, Validation, and Interpretation of Satellite Oceanographic) dataset, (http://www.aviso.oceanobs.com/) with two descending (i.e. cross-shelf) tracks falling inside the MAB (black dashed lines in Fig. 2). For direct comparison, the model-simulated SSHA is sampled at the same time interval as the along-track satellite data, which is 9.9 days (note the tidal signals are deducted from both model result and the satellite data). The Hovmöller diagrams of the satellite-observed and model-simulated SSHA along the two selected tracks are shown in Fig. 4. Along the two tracks, both AVISO and ROMS indicate that large SSHA variation, with an increasing magnitude of up to 0.5 m, occurs offshore toward deeper waters where energetic meanders and eddies often exert strong spatial-temporal influence on the shelf circulation. Although the model misses some of the fine-scale sea level structures, it captures the seasonal and interannual variability of the sea level reasonably well.

In summary, the abovementioned model-observation comparisons suggest that our model simulation is reliable for understanding the mean state, seasonal and interannual variability over the MAB shelf and slope regions.

4. Mean state

Even though the focus of this study is the interannual variability of the MAB shelf/slope front and jet system, it is still necessary to examine its mean state and climatological seasonal variations to gain an understanding of the fundamental dynamics. In this section we will present an analysis based on the model results form experiment REAL.

4.1. Annual mean

The principal circulation features of the modeled mean surface circulation are shown in Fig. 5. Consistent with the schematic of Fig. 1 (as drawn from observations), the continental shelf circulation includes an inflow from the Scotia Shelf to Gulf of Maine, a cyclonic circulation in the Gulf of Maine, an anti-cyclonic circulation on the Georges Bank, and a southwestward along-shelf flow over the MAB. Over the shelfbreak to continental slope (bounded by the isobaths from 100 to 1000 m) the shelf-edge current carries southwestward outflow along the Scotia Shelf and upper slope, with a small branch entering the Gulf of Maine through the Northeast Channel, and a larger branch directly merging with the clockwise gyre over the Georges Bank creating a narrow but intensified jet equatorward along the MAB shelfbreak. The shelf waters and shelfbreak jet converge with the northward moving Gulf Stream near Cape Hetaeras, then turns northeastward further offshore of Cape Hatteras.

In order to illustrate the mean structure of the along-shelf jet, we construct two-dimensional cross-shelf fields of the along-shelf velocity and hydrography (Fig. 6) by performing along-shelf averaging in the southern New England region (shaded area in Fig. 5). The mean along-shelf velocities are mostly southwestward and range from zero to about 0.25 m s^{-1} in the center of the shelfbreak jet with a surface intensified velocity structure spanning the 100–200 m isobaths (Fig. 6a). At the shelfbreak the upward tilted salinity front, centered on the 34.5 isohaline, extends all the way to the surface. Unlike the temperature, which exhibits a strong seasonal thermocline, the shelfbreak salinity front is a persistent feature throughout the year, with a gradient of about 1 PSU over 10–40 km. In previous studies, more often than not, the 34.5 isohaline is used as a distinct separation in properties between the shelf and slope water and to indicate the shelfbreak front (Beardsley and Flagg, 1976; Linder and Gawarkiewicz, 1998; Linder et al., 2006; Chen and He, 2010). It is worth-noting that, over the outer shelf and shelfbreak, the cross-shelf temperature and salinity gradients have opposite contributions to the density gradients (Fig. 6b,c). It is the salinity front that creates a strong density gradient that is primarily responsible for the strong shelfbreak jet.

The momentum budget analysis provides further insight into the shelf/slope flow. Here we focus on the momentum budget in the cross-shelf direction in order to identify the fundamental

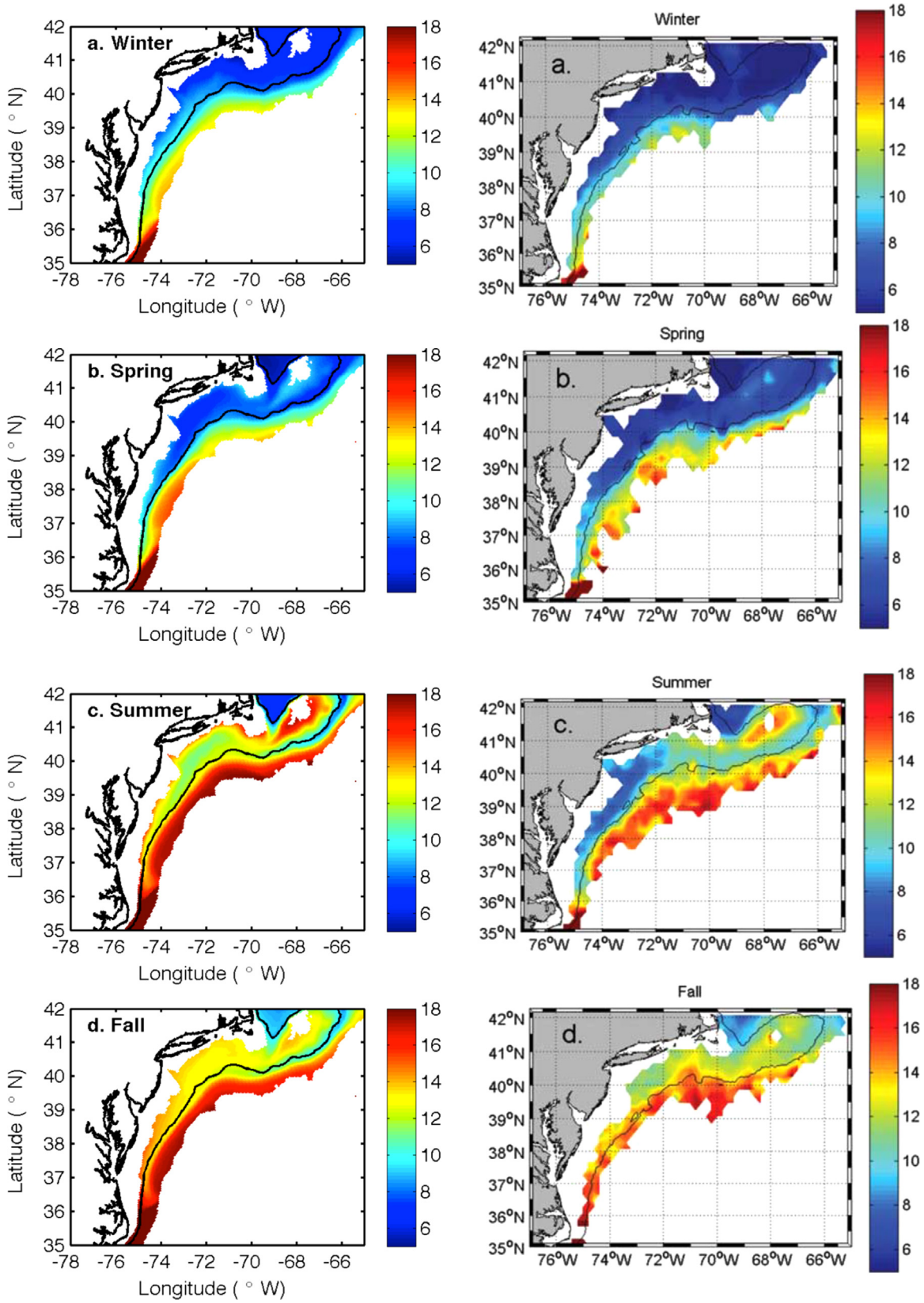

Fig. 3. (a) The comparison between the model solutions for seasonal mean temperatures (left column) and the climatology produced by Linder et al. (2006) (right column) at mid-depth (40–55 m) in (a) winter, (b) spring, (c) summer, and (d) fall. Black line indicates 100 m isobath. (b) As in Fig. 3a, but for salinity.,

dynamical balances dominating the along-shelf jet. Fig. 7 illustrates the cross-shelf distributions of the Coriolis force, the horizontal pressure-gradient force (PGF), the viscosity term (horizontal and vertical diffusion combined), and nonlinear advection term (horizontal and vertical advection combined), and these terms are all along-shelf averaged within the shaded area in Fig. 5. As expected, the Coriolis force and pressure-gradient force are dominant terms and they nearly balance each other. The viscosity

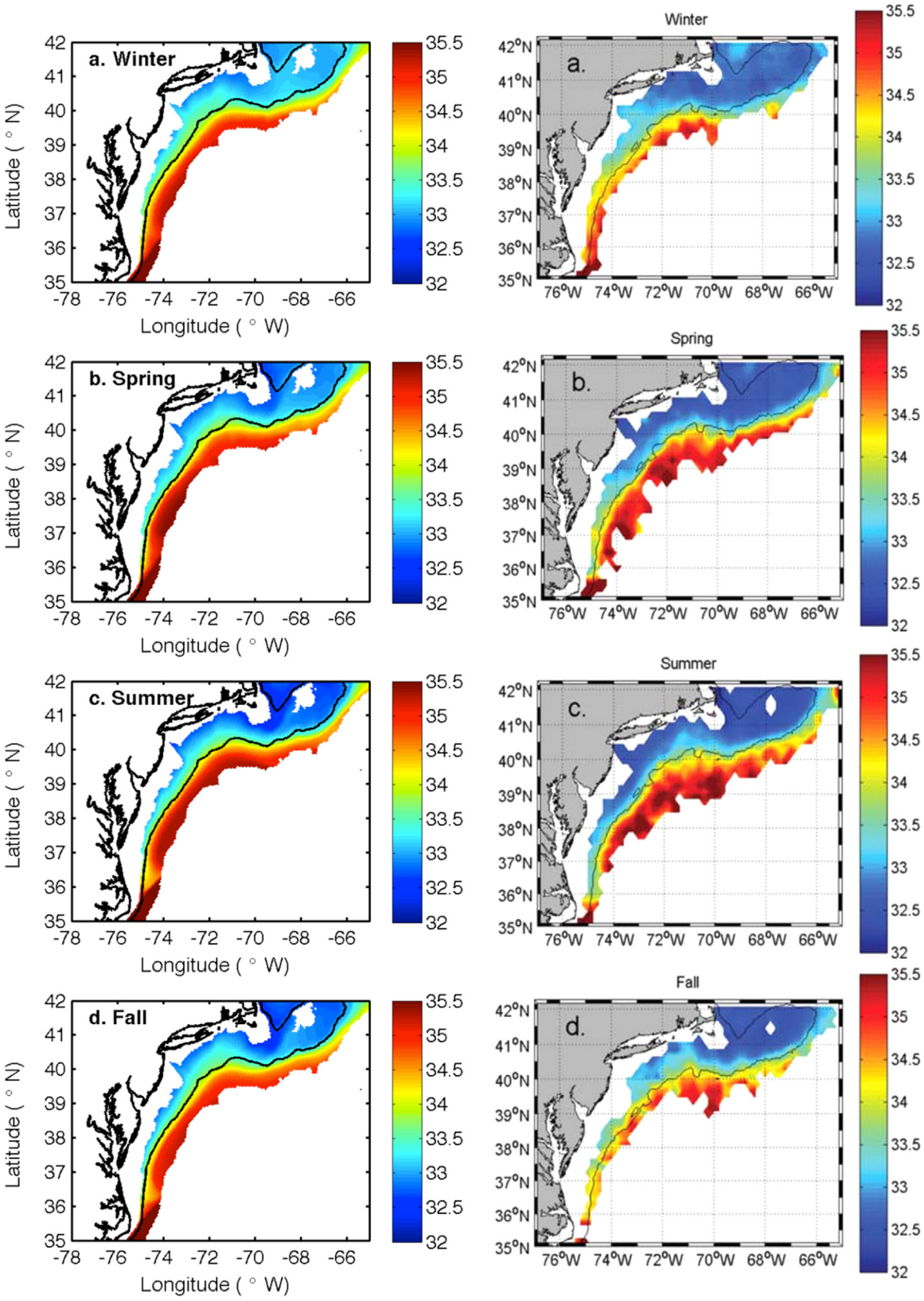

Fig. 3. (*continued*)

term is relatively strong on the shelf near the bottom boundary, while the nonlinear advection term is relatively strong over the shelfbreak due to the energetic currents. But both viscosity and nonlinear advection terms are one order of magnitude weaker than the leading geostrophic terms. This indicates that the along-shelf jet is in geostrophic balance to leading order, which is consistent with previous studies (e.g., Linder and Gawarkiewicz, 1998; Chen and He, 2010; Zhang et al., 2011).

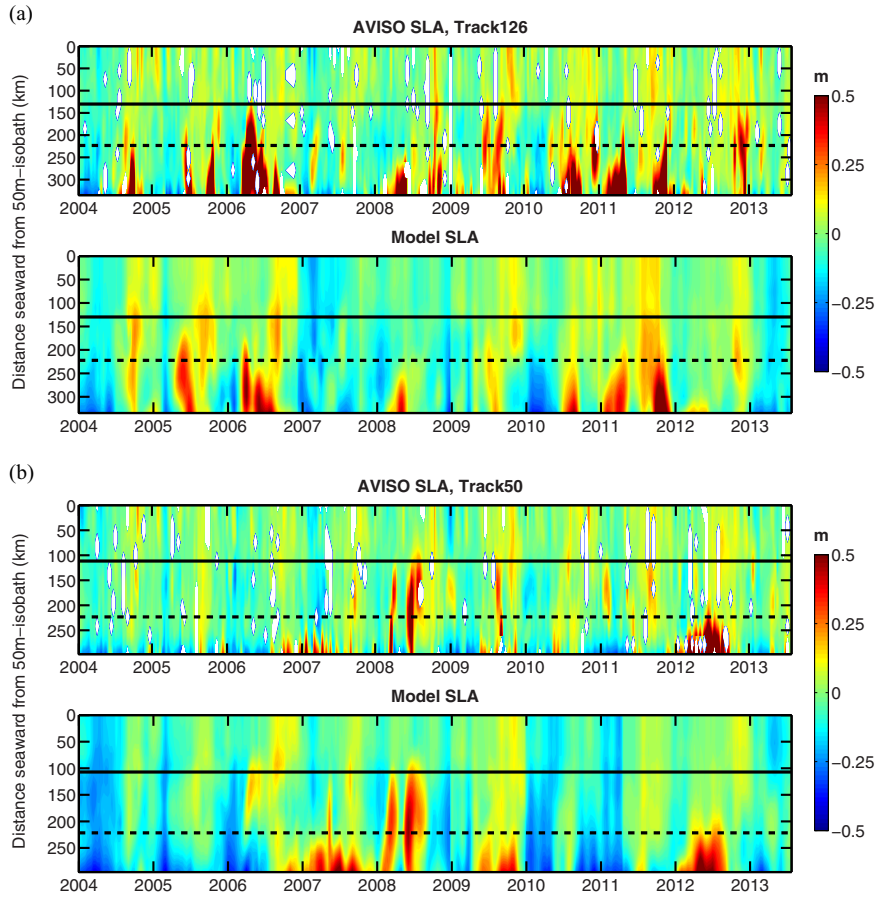

Fig. 4. Hovmöller diagrams of satellite-observed (upper panel) and model-simulated (lower panel) cross-shelf transect of SSHA (unit: m) along (a) Track-126; (b) Track-50 from Jan. 2004 to Dec. 2013. The black solid line and the dash line indicate the 1000 and 3000 m isobaths, respectively.

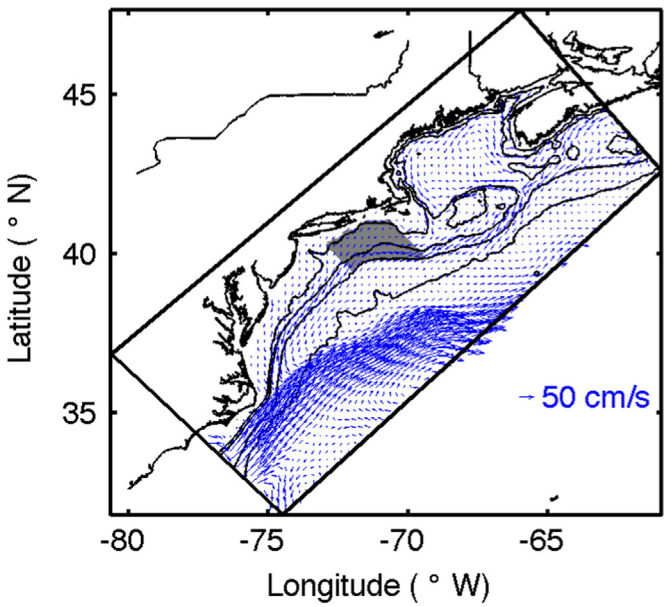

Fig. 5. Mean-state surface velocity from experiment REAL. The black box is regional-scale ROMS model domain and the shaded area denotes the region where the along-shelf average is conducted. The 50, 100, 1000, and 3000 m isobaths are also shown.

4.2. Seasonal means

The seasonal means of the along-shelf velocity are illustrated in Fig. 8. Henceforth, four typical months February, May, August and November are used to represent the four seasons. The shelfbreak jet accelerates in the fall and is strongest in winter with a maximum mean speed of over 0.35 m s^{-1} and a width of 30 km. This is also the time when the jet core shifts offshore within a thin surface trapped layer (shallower than 60 m). In May, the jet core starts to move onshore and the poleward current is intensified as a subsurface feature seaward of the shelfbreak. The intensity of the shelfbreak jet is significantly reduced in August with mean speeds less than 0.2 m s^{-1}, and the reduced southwestward flow expands to a width of 50–60 km, consistent with the observation of Flagg et al. (2006). As discussed earlier, the along-shelf jet is nearly in thermal wind balance. The seasonal variability of the along-shelf jet can largely be attributed to the seasonal changes in the cross-shelf density gradient. Several sources of seasonal variation in the cross-shelf density structure, like the tidal mixing front over Georges Bank, surface heat flux, and spring runoff near the MAB coast were identified and have been studied in detail within different sub-regions over the MAB (e.g., Flagg, 1987; Shearman and Lentz, 2003; Rasmussen et al., 2005; Zhang et al. 2009). In the following, we will primarily focus on the interannual variability of the along-shelf jet.

5. Interannual variability and its origins

5.1. Along-shelf transport

Our 10-year-long numerical simulations provide a unique opportunity to investigate the interannual variability in both circulation and hydrography field. A straightforward way to identify interannual variability is through a time series of along-shelf

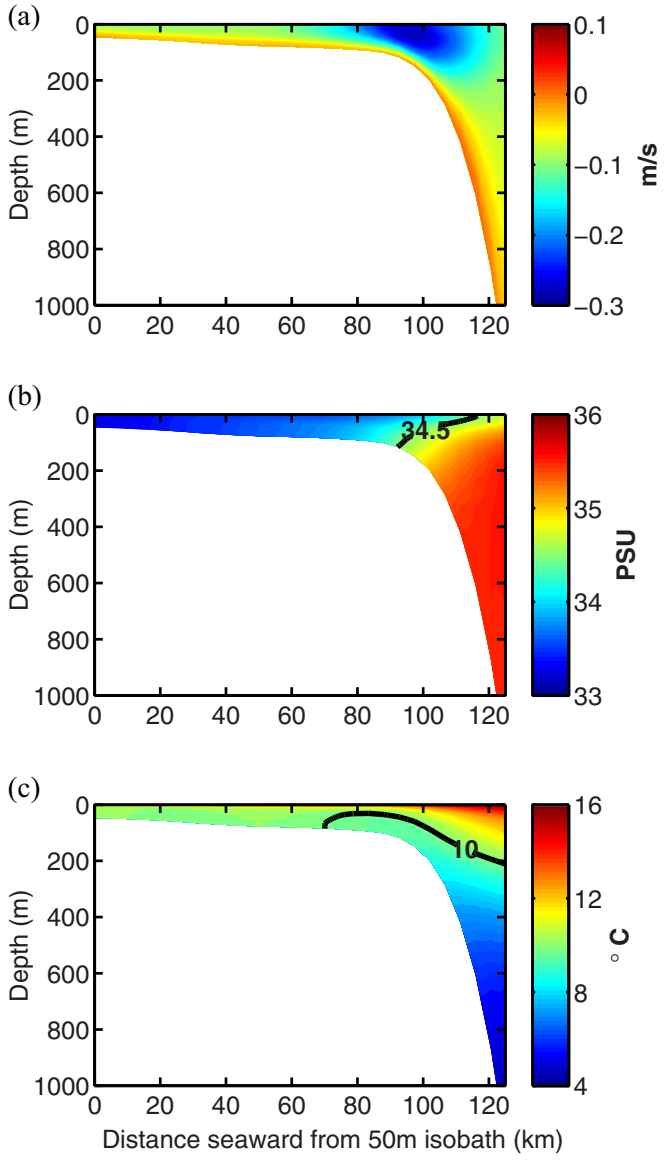

Fig. 6. Mean-state along-shelf (a) velocity (negative values indicate southwestward direction, $m\,s^{-1}$); (b) salinity (black contour highlights 34.5 PSU isohaline); (c) temperature (black contour highlights 10 °C isothermal) in the southern New England shelf/slope area (shaded area in Fig. 5).

transport. Previous studies (e.g., Lentz, 2008a, 2008b; Chen and He, 2010; Zhang et al., 2011) presented the annual and seasonal mean along-shelf flows in the MAB region are all southwestward, increasing gradually in the offshore direction and reaching the peak values at the shelfbreak while never extending to the neighboring continental slope deeper than 1000 m depth. To quantify the interannual variability of the along-shelf transport of the shelfbreak jet, we select a cross-shelf section between 100 and 1000 m isobaths (T_1 in Fig. 1) that represents the upper bound of the northern MAB, and calculate the monthly averaged upper water column transports from experiment REAL by integrating the monthly averaged along-shelf velocity from the surface to 200 m depth. The result is represented as a black line labeled REAL in all of the three panels of Fig. 9. Clearly, the obtained along-shelf transport exhibits significant interannual variability during the 10-year simulation, with the magnitude of the variation about 3 Sv. In particular, two features are notable: (1) the southwestward along-shelf transport is higher during wintertime both in 2009 and 2010 than other years and, 2) there are three significant reversals of southwestward along-shelf transport that occur in 2004 October, 2005 September and 2007 July. Two questions naturally arise. (1) What is the origin of the interannual variability of the along-shelf transport in the MAB region, i.e., is it due to the influence of local surface forcing or of remote forcing? (2) If it is the latter, what are the contributions of the upstream and offshore forcing? These two questions will be addressed in the following section.

5.2. Origins of the interannual variability

We now focus on the comparisons of the along-shelf transport along the T_1 transect between the REAL experiment and the other five experiments described in Section 2. In Fig. 9a, there is hardly a discernible difference of along-shelf transport after controlling the surface wind with climatology, and only subtle distinctions after replacing both surface wind and buoyancy forcing with their climatologies. We can therefore confidently conclude that the interannual variability along transect T_1 does not appear to be caused by local atmospheric momentum or buoyancy forcing but rather must be due to processes on a much larger scale.

Focusing now on the impact of remote forcing, we compare experiments REAL and OBCs (Fig. 9b). The interannual variability of the along-shelf transport across T_1 (REAL) disappears in OBCs (which only retains the climatological open boundary forcing; see Table 2). The seasonal cycle remains in OBCs with a regular range of 0.8 Sv between its winter maximum and summer minimum. This further supports our previous conclusion that it is the variability of the remote forcing that accounts for the interannual variability of the along-shelf front/jet system along this transect.

We next move on to compare the along-shelf transport between experiments REAL, UPSTREAM (interannual variability of the upstream forcing is removed) and OFFSHORE (interannual variability of the offshore forcing is removed). The transports in both experiments UPSTREAM and OFFSHORE show significant departures from that in REAL (Fig. 9c), suggesting that both the upstream and offshore processes have significant impacts on the interannual variability of the along-shelf transport in the MAB region. In particular, the transport in winters of 2009 and 2010 are reduced in UPSTREAM as compared with REAL, suggesting that in reality the upstream process (Labrador Current) very likely causes the high transport in winters of 2009 and 2010. In experiment OFFSHORE, the three periods of reversed along-shelf transport before 2009 completely vanish, implying the physical process associated with the Gulf Stream might be responsible for the reversed along-shelf transport. In the following, we will better detail the upstream influence from the Labrador Current and the offshore effects from the Gulf Stream.

6. Influence of remote processes

6.1. The Labrador Current

To confirm that the high along-shelf transport in winters of 2009 and 2010 is due to the intrusion of the Labrador Current, we examine the hydrography in the MAB region and the flow structure at the northern boundary of the model domain. In the following analysis, we mainly present the analysis based on the results in 2009. Fig. 10 shows the 10-year averaged wintertime temperature and salinity fields at 50 m depth from experiment REAL for the entire region (Fig. 10a,c) and the anomalies in 2009 wintertime (Fig. 10b,d). The anomalies are obtained by subtracting the 10-year averaged hydrographic fields from the hydrographic fields in 2009. Fig. 10a,c clearly reveals the cool and fresh shelf water as compared with the slope water. The shelf/slope front acts as a boundary between these two water masses in the narrow

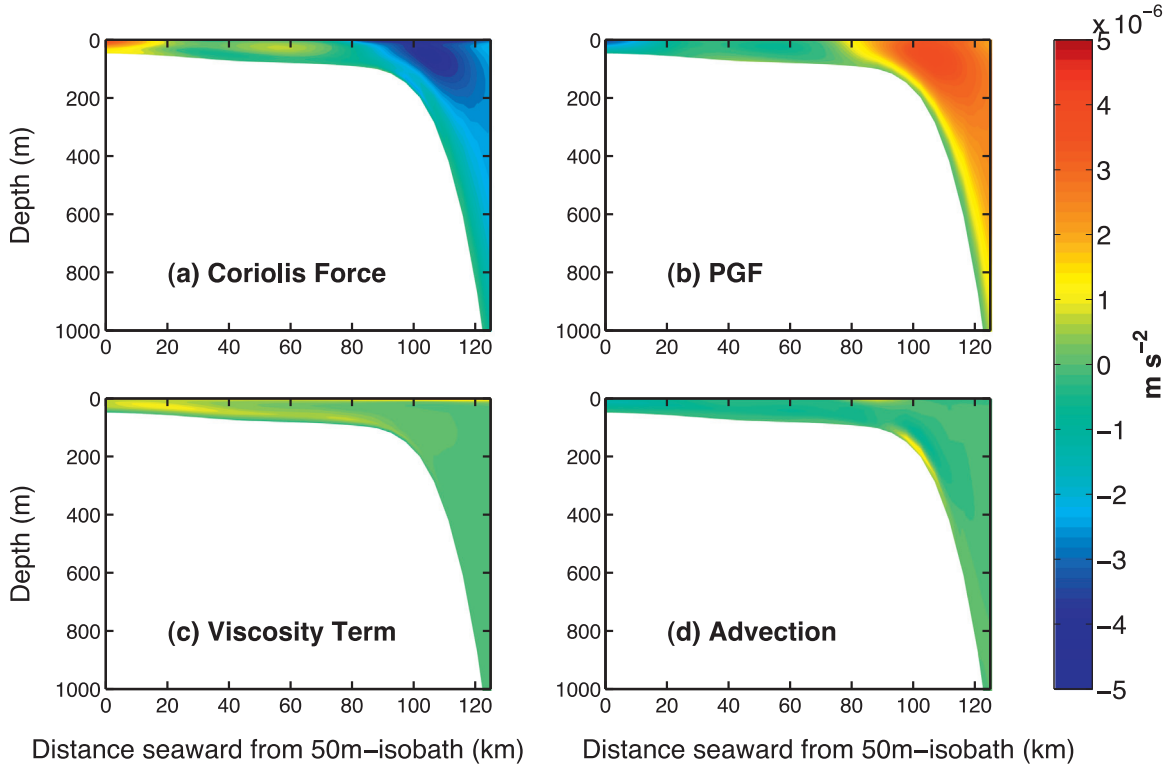

Fig. 7. Cross-shelf distribution of the along-shelf momentum budget terms: (a) the Coriolis force, (b) the PGF, (c) the viscosity and (d) the nonlinear advection terms.

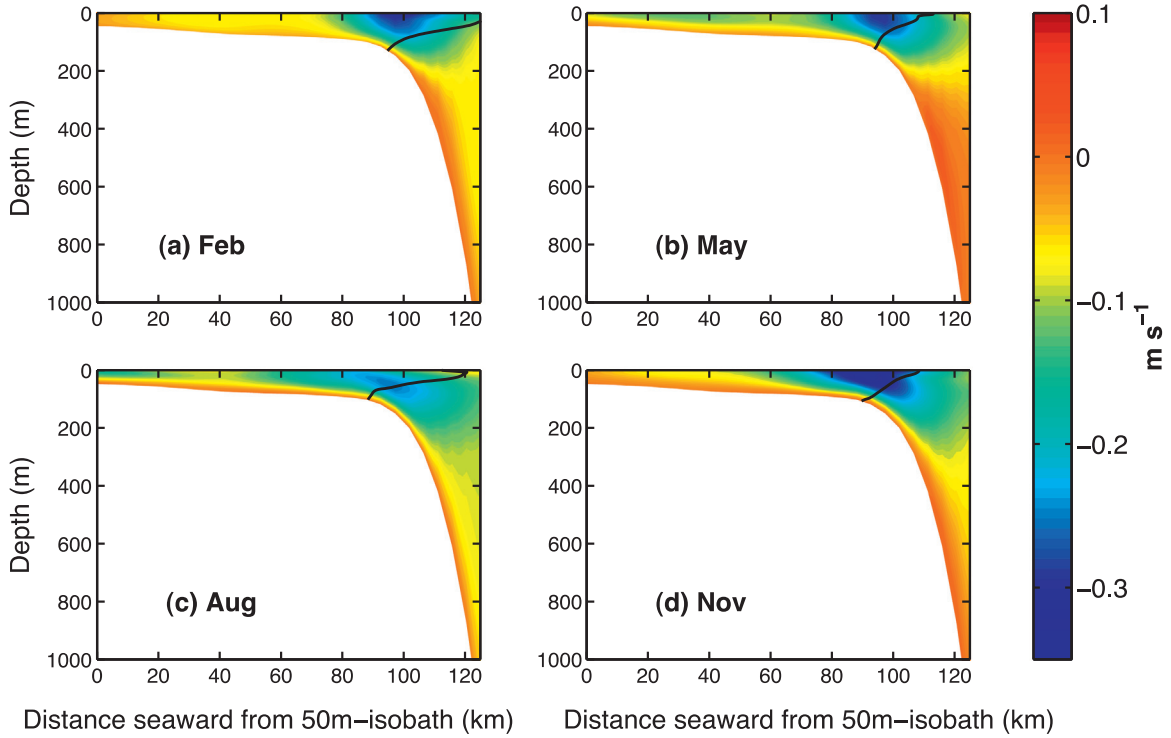

Fig. 8. Cross-shelf distributions of the along-shelf velocity (represented by the colors; negative values indicate southwestward direction) and 34.5 PSU isohaline (black contour, indicating the shelfbreak front) averaged in the southern New England shelf/slope area in (a) February, (b) May, (c) August, and (d) November. (For interpretation of the references to color in this figure legend, the reader is referred to the web version of this article.)

transition region between the 100 and 1000 m isobaths. In 2009, significant negative anomalies in the temperature and salinity fields with magnitudes up to −3 °C and −1 PSU, respectively, dominate the MAB shelf/slope region. Such hydrographic anomalies are spatially coherent from the Scotia Shelf to Cape Hatteras. The abnormal cold and fresh water in our model domain originates from the north, as far as the Labrador Sea, implying that source locates at the north boundary of the model domain.

Fig. 11 compares the climatological (10-year averaged) and 2009 wintertime hydrography and the along-shelf velocity at the

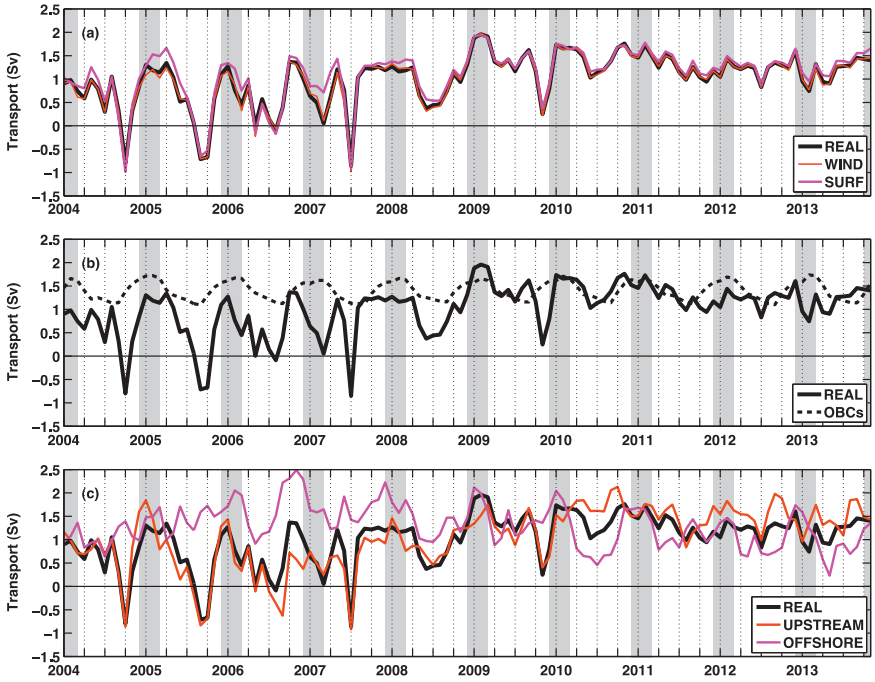

Fig. 9. Time series of the along-shelf transport cross T_1 transect in different experiments: (a) REAL, WIND and SURF; (b) REAL and OBCs; (c) REAL, UPSTREAM and OFFSHORE.

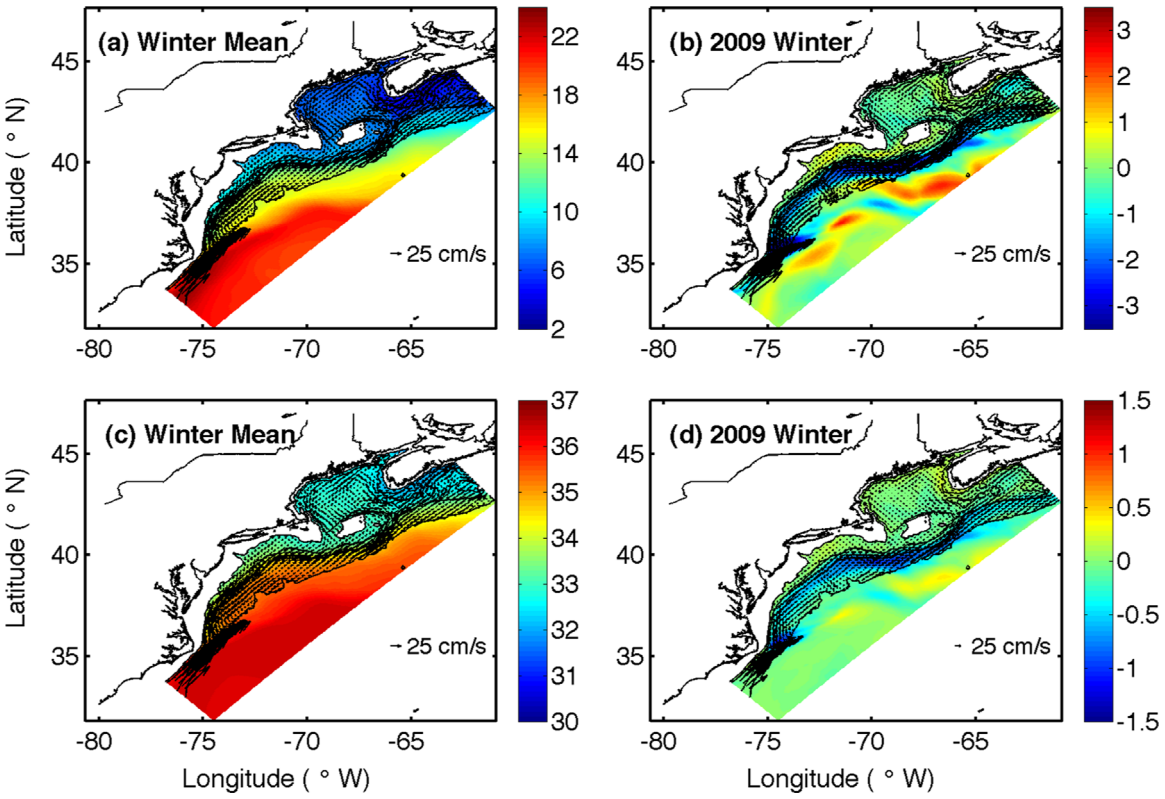

Fig. 10. Mid-depth (50 m) distribution of (a) 10-year averaged winter temperature (color, unit: °C) and surface velocity (vectors) and (b) temperature anomaly for the 2009 winter (color, unit: °C) and surface velocity (vectors) from experiment REAL. (c) and (d) are for salinity (color, unit: PSU) and surface velocity (vectors). The 50, 100, 1000, and 3000 m isobaths are also shown. (For interpretation of the references to color in this figure legend, the reader is referred to the web version of this article.)

north boundary of the model domain. The basic structure of the climatological wintertime hydrography (Fig. 11a, c) shows that temperature and salinity values generally increase with depth and distance offshore, with the largest horizontal gradients occurring on the inner shelf and at the shelf edge. This is consistent with the long-term observations of hydrographic properties on the Halifax section by Loder et al. (2003). Over the upper continental slope, a wedge of relatively fresh and cold upper-layer shelf water overlie two types of slope waters, which are identified by Pershing et al. (2001): (1) a layer of warm slope water (temperature of 8–12 °C and salinity of 34.7–35.5 PSU) and, (2) Labrador slope water (4–8 °C, 34.3–35.3 PSU) at intermediate depth. Below these is the

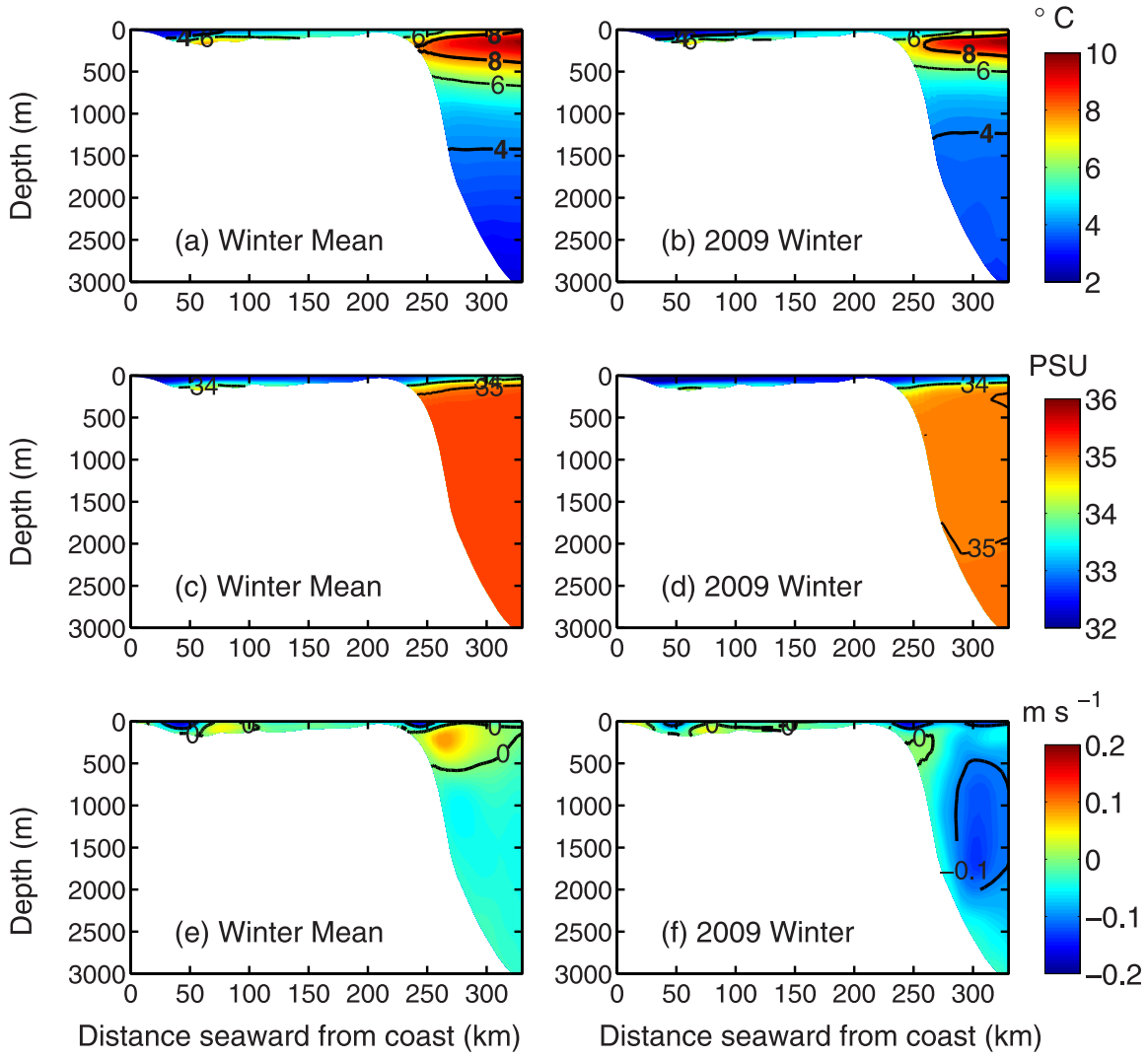

Fig. 11. Comparison between the winter-averaged physical fields in the climatological state (left) and in 2009 (right) along the northeastern boundary of the model domain. (a,b): temperature, with 4 °C and 8 °C isothermals highlighted; (c,d) salinity, with 34 and 35 PSU isohalines highlighted; (e,f) along-shelf velocity, with the negative values indicating a southwestward current.

so-called classical Labrador sea water with a characteristic potential temperature of 3 °C and a salinity of 34.88 PSU (Smethie et al., 2000). The dominant features of the velocity fields along the northeast boundary are surface-intensified southwestward flows on both the inner shelf (the Nova Scotia Current described by Drinkwater et al., 2002) and near the shelf edge over the upper slope, which is part of the downstream remnant of the shelf-edge Labrador Current (Loder et al., 1998). The subsurface northeastward flows are identified as the slope current that is strongly influenced by Gulf Stream meanders and anti-cyclonic warm-core rings (Joyce, 1991). The striking feature in the winter of 2009 is the relatively strong southwestward current (Fig. 11f). Associated with this current is the relatively cold and fresh water (Fig. 11b, d). All these features reveal the intrusion of the Labrador Current into the model domain from the north boundary in 2009 wintertime. Similar behavior of Labrador Current also occurred in 2010 wintertime (not shown).

6.2. *The warm core rings*

The close proximity of the Gulf Stream in southern New England results in a large number of meanders and anti-cyclonic warm core rings (WCRs) each year that, from time to time, impinge upon the continental slope in the MAB. These rings could generate significant temporal and spatial variability in the currents, i.e. reversing the flow at the shelfbreak (Beardsley et al., 1985), pulling streamers of shelf water into the interior (Joyce, 1991), or stimulating shear instabilities due to the enhanced horizontal velocity gradients of the shelfbreak jet (Ramp et al., 1983).

During the 10-year simulation, there are three significant reversals of southwestward along-shelf transport on the shelf/slope: 2004 October, 2005 September and 2007 July. For each reversal, we plot the latitude/longitude structure of the surface speed and velocity (Fig. 12). An anticyclonic ring circulation occurred during each period between 37.5 and 40.5°N in the vicinity of the 1000 m isobath just south of Georges Bank, which has been well documented as a place with maximum ring activity (Chaudhuri et al., 2009a,b), and impacted the circulation further to the north by interacting with the shelf/slope front. To validate the modeled eddy activity, we retrieve daily snapshots of satellite altimetry observed sea level anomalies (SLA) as a more reliable proxy for the presence and duration of warm core rings (WCRs). The gridded SLA fields with spatial resolution of $1/4^\circ \times 1/4^\circ$ are obtained from AVISO based on the Jason-1 and Jason-2 missions. Consistent with the numerical simulations, the daily snapshots reveal notable WCRs with a diameter of more than 150 km in the same location

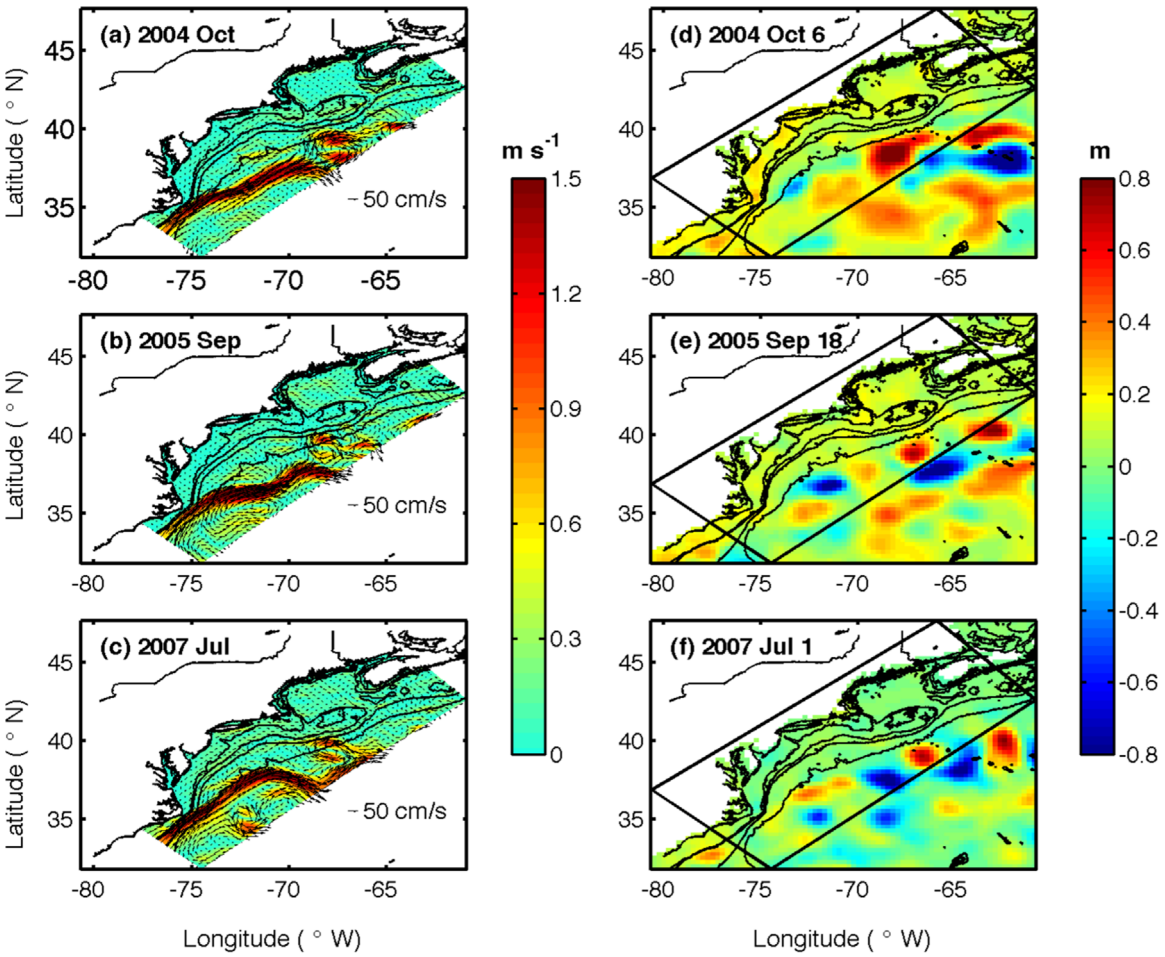

Fig. 12. (Left column) Monthly mean surface velocity (vectors) and current speed (color) for (a) 2004 October, (b) 2005 September and (c) 2007 July. (Right Column) Daily snapshots of gridded AVISO SLA on (d) Oct 6, 2004, (e) Sep 18, 2005 and (f) Jul 1, 2007. The 50, 100, 1000, and 3000 m isobaths are shown in all figures. (For interpretation of the references to color in this figure legend, the reader is referred to the web version of this article.)

(Fig. 12, d–f). Actually, the similarity of these three periods is that the WCR features are present almost without change for a period longer than 10 days; a time-longitude plot (not shown) indicates their westward propagation speed is very slow at $\sim$3 km day^{-1}.

The along-shelf velocity and isopycnals across the T_1 transect during the abovementioned three reversal periods are presented in Fig. 13. As expected, the southwestward jet is fully replaced by northeastward currents associated with the WCRs. To leading order, the geostrophic and hydrostatic along-shelf flow obeys the thermal-wind balance; the frontal density gradient is in balance with the vertical shear of along-shelf velocity. The presence of offshore eddies from the shelfbreak to the slope affects the direction and the magnitude of the along-shelf velocity by reversing the cross-shelf density gradient.

7. Interpentadal variability

In this section we focus on the change of the along-shelf transport in our model simulations between the pentads 2004–2008 and 2009–2013. Besides the T_1 transect discussed earlier, we select two more cross-shelf sections in the model domain, noted as T_2, which is located in the southern MAB area, and T_3, which is close to the northern boundary of the regional model domain, respectively (Fig. 1). Using the same analysis as for the T_1 transect, we calculate the monthly averaged transports cross T_2 and T_3 from experiment REAL (black heavy lines in Fig. 14) and OBCs (black dashed lines) in the upper water column. For each transect the time series of the along-shelf transport anomaly is obtained by subtracting the results of the experiment OBCs from that of experiment REAL (black thin lines). Furthermore, the pentadal mean values of along-shelf transport during 2004–2008 (blue lines) and 2009–2013 (red lines) are also obtained. Interestingly, for both of the T_1 and T_2 transects, the along-shelf transport during 2004–2008 is dominated by negative anomalies, however, this is not the case for the T_3 transect. The 5-year averaged transports of T_1 and T_2 show a significant (approximately 100%) increase between the pentads 2004–2008 and 2009–2013. In contrast, there is hardly any discernible increase for T_3 between these two pentads. This indicates that the along-shelf transport is featured with significant interpentadal variability during our 10-year model simulation and such variability is very likely due to the variability of the Gulf Stream.

Next we explore the variations of the Gulf Stream during the 10-year model simulation. In particular, we focus on the migration of the northern edge of the Gulf Stream based on the modeled sea surface height (SSH) fields. Taylor and Stephens constructed a measure of the latitude of the north edge of the Gulf Stream, known as the Gulf Stream north wall (GSNW) index based on observations (Taylor, 2011). By mapping their climatological path of the GSNW (black dots in Fig. 15) with our simulated climatological SSH, we find the 35-cm SSH contour is most close to the observed Gulf Stream north wall (white lines in Fig. 15). Therefore we choose the 35-cm SSH contour as a proxy for the Gulf Stream

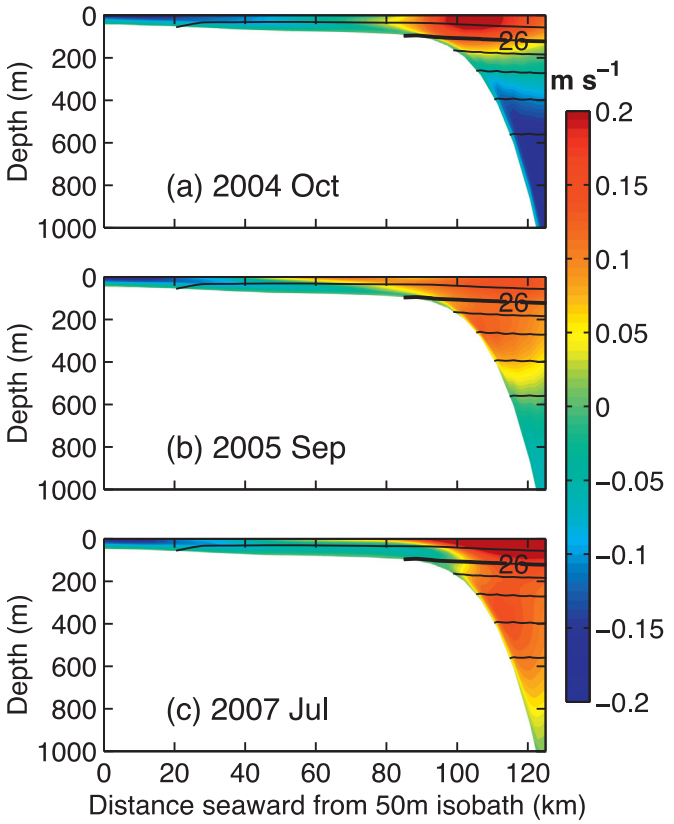

Fig. 13. Cross-shelf distributions of the along-shelf velocity (represented by the colors, unit: m s^{-1}; negative values indicate southwestward) and the potential density (represented by the black contours) along T_1 section in (a) October 2004, (b) September 2005 and (c) July 2007. (For interpretation of the references to color in this figure legend, the reader is referred to the web version of this article.)

northern edge. Interestingly, during 2004–2008, the Gulf Stream northern edge (red contours in Fig. 15) is apparently north of its mean position; while during 2009–2013, the Gulf Stream shifts offshore and remains close to its mean position. To understand how the migration of Gulf Stream north wall affect the inter-pentadal variability of the along-shelf transport (Fig. 14), we derive

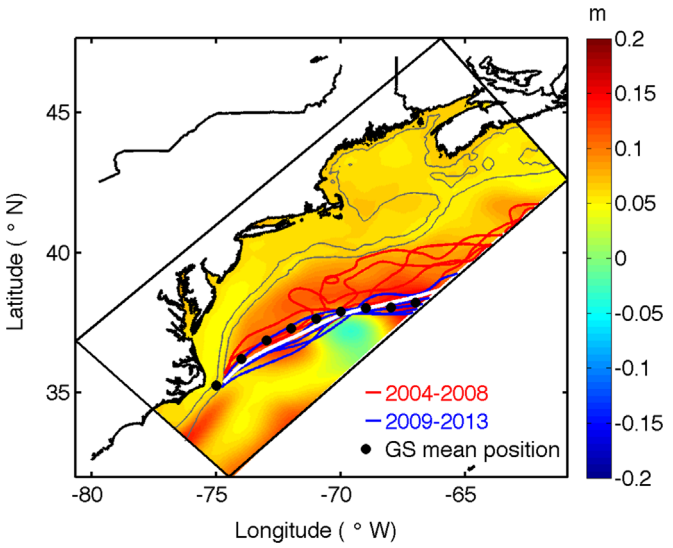

Fig. 15. The spatial distribution of the SSH anomaly during 2004–2008 (colors), which is obtained by subtracting the 10-year averaged SSH from the 2004–2008 averaged SSH. The climatological mean locations of the Gulf Stream North Wall from Taylor (2011) are denoted by the black dots. The 10-year averaged 35 cm SSH from experiment REAL is highlighted by the white contour, and the annual averaged 35 cm SSH during 2004–2008 (2009–2013) are represented by the red (blue) contours. The 100 m and 1000 m isobaths are shown by thin black lines. (For interpretation of the references to color in this figure legend, the reader is referred to the web version of this article.)

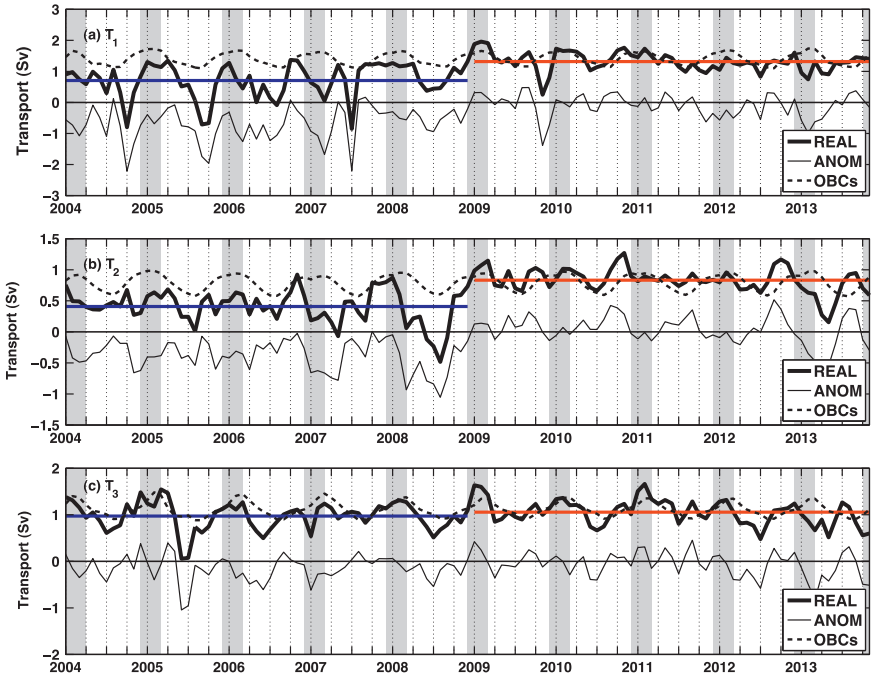

Fig. 14. Time series of the along-shelf transport integrated between 100 and 1000 m isobaths in the upper 200 m water depth from experiment REAL (black heavy lines) and experiment OBCs (black dashed lines) along (a) T_1, (b) T_2 and (c) T_3. The transport anomalies (black thin lines) are calculated by subtracting OBCs from REAL. The five-year averaged along-shelf transports during 2004–2008 (2009–2013) are represented by the blue (red) lines in (a)–(c). Positive values indicate southwestward flow. The shaded areas denote winter months, which are December, January, February and March. (For interpretation of the references to color in this figure legend, the reader is referred to the web version of this article.)

the SSH anomaly during the pentad 2004–2008 (color in Fig. 15), which is obtained by subtracting the 10-year averaged SSH field from the 5-year average during 2004–2008. In the MAB region, the SSH anomaly increases from shelf to slope, creating a cross-shelf pressure gradient opposing the along-shelf jet, and thus leads to the reduction of the along-shelf transport as well as the jet strength during 2004–2008. This idea is consistent with Ezer et al. (2013). They indicated that the variation of the Gulf Stream path and strength could directly affect the strength of the slope current through a 'dynamic sea level change' mechanism. In particular, Ezer et al. (2013) pointed out that when the Gulf Stream is farther offshore (onshore), the southward slope current is enhanced (reduced) (see their Fig. 2), which is in agreement with our finding.

In our regional model simulation, the variability of the Gulf Stream is passed from the basin-scale HYCOM simulation. The mechanism causing the variation of Gulf Stream path during our model simulation (2004–2013) and particularly the shift of Gulf Stream north wall around the year of 2009 is uncertain. A detailed examination is beyond the scope of this study and below we just propose two plausible physical explanations. The transport of AMOC was reported reduced by 30% during 2009–2010 (McCarthy et al., 2012). It is possible that with weaker AMOC, the Gulf Stream was also weaker and it shifted farther away offshore, causing enhanced along-shelf transport. Previous studies also suggested that the North Atlantic Oscillation (NAO) could have a large impact on the Gulf Stream. For example, the position of the Gulf Stream north wall was observed to move northward (southward) during positive (negative) phases of the NAO with a lag of about 1–2 years (Rossby and Benway, 2000). During the period of our model simulation, the NAO index shifts to negative value in winter 2008/2009 and has a record negative value in winter 2009/2010 (Osborn, 2011). The variation of Gulf Stream around the year of 2009 path might also be caused by to the change of NAO phase.

8. Summary

This study sets out to better understand the interannual variability of the along-shelf transport and water properties in the MAB region. ROMS is employed to simulate the front/jet system along the U.S. Northeast continental shelf/slope region for the decade from January 2004 to December 2013. The region model is forced by realistic atmospheric and tidal forcing and river runoff, and the open boundary forcing is derived from a global eddy-resolving numerical simulation provided by HYCOM/NCODA. Model results are first compared with observations and then a detailed investigation of the mean state and seasonal variability of MAB shelf/slope circulation and hydrography is presented. Term-by-term analyses of momentum equation confirm that the shelfbreak jet is essentially in thermal wind balance.

Special attention has been given to the origins of interannual variability of the circulation, especially the along-shelf transport in the northern MAB. Results from a series of process-oriented experiments indicate that remote forcing from the open boundaries plays a more important role than local atmospheric forcing. More specifically, the upstream influence of the Labrador Current is the major source leading to an increase of along-shelf transport in the MAB in the winters of 2009 and 2010. By contrast, the anti-cyclonic warm core rings associated with the Gulf Stream reduce and even reverse the along-shelf transport. We also find that the along-shelf transport in the 10-year simulation is featured with an interpentadal variability, that is the time-averaged transport during 2004–2008 is significantly lower than 2009–2013. The underlying mechanism is that the Gulf Stream was able to maintain an anomalous northerly path during 2004–2008 and the Gulf Stream returns to its climatological position during 2009–2013.

The along-shelf jet is the dominant physical feature in the MAB region. The interannual-to-interpentadal variability of the along-shelf transport associated with the jet could lead to a change of coastal water environment and the marine ecosystems, e.g. primary productivity and the biological export of carbon (Drinkwater et al., 2002). Future observational/modeling effort is recommend for further understanding the long-term variability of the front/jet system in the MAB shelf/slope and its impacts on the coastal environment.

Acknowledgements

The research was funded by NSF RI EPSCoR(S000216). Dr. Luo acknowledges the support of the National Natural Science Foundation of China (41376009) and the Joint Program of Shandong Province & National Natural Science Foundation of China (U1406401). We thank the ROMS group at Rutgers University for their valuable suggestions on the model configuration in this work. We also want to the two anonymous reviewers for providing the insightful comments that significantly improved this paper.

References

Beardsley, R.C., Flagg, C.N., 1976. The water structure, mean currents, and shelf water/slope water front on the New England Continental shelf, Memoires Societé Royale des Sciences de Liége, 6e serie, tome **X**, pp. 209–255.

Beardsley, R.C., Chapman, D.C., Brink, K.H., Ramp, S.R., Schlitz, R., 1985. The Nantucket Shoals Flux Experiment (NSFE79), Part 1: A basic description of the current and temperature variability. J. Phys. Oceanogr. 15, 713–748.

Biscaye, P.E., Flagg, C.N., Falkowski, P.G., 1994. The shelf edge exchange processes experiment, SEEP-II: an introduction to hypotheses, results and conclusions. Deep-Sea Res. II 41, 231–252. http://dx.doi.org/10.1016/0967–0645(94)90022-1.

Chaudhuri, A.H., Gangopadhyay, A., Bisagni, J.J., 2009a. Inter-annual variability of Gulf Stream warm-core rings in response to the North Atlantic Oscillation. Cont. Shelf Res. 29, 856–869.

Chaudhuri, A.H., Bisagni, J.J., Gangopadhyay, A., 2009b. Shelf water entrainment by Gulf Stream warm-core rings between 75°W and 50°W during 1978–1999. Cont. Shelf Res. 29, 393–405.

Chen, K., He, R., 2010. Numerical investigation of the Middle Atlantic Bight shelf-break frontal circulation using a high-resolution ocean hindcast model. J. Phys. Oceanogr. 40, 949–964.

Dickey, T., Williams III, A.J., 2001. Interdisciplinary ocean process studies on the New England shelf. J. Geophys. Res. 106, 9427–9434. http://dx.doi.org/10.1029/2000JC900155.

Drinkwater, K.F., Petrie, B., Smith, P.C., 2002. Hydrographic variability on the Scotia Shelf during the 1990s, NAFO SCR Doc. 02/42, 16pp.

Ezer, T., Atkinson, L.P., Corlett, W.B., Blanco, J.L., 2013. Gulf Stream's induced sea level rise and variability along the U.S. mid-Atlantic coast. J. Geophys. Res. Ocean. 118, 685–697. http://dx.doi.org/10.1002/jgrc.20091.

Ezer, T., 2015. Detecting changes in the transport of the Gulf Stream and the Atlantic overturning circulation from coastal sea level data: The extreme decline in 2009–2010 and estimated variations for 1935–2012. Glob. Planet. Chang. 129, 23–36.

Flagg, C.N., 1987. Hydrographic structure and variability. Georges Bank. In: Backus, R.H., Bourne, D.W. (eds.). MIT Press, Cambridge, Massachusetts, pp. 108–124, .

Flagg, C.N., Dunn, M., Wang, D.-P., Rossby, H.T., Benway, R.L., 2006. A study of the currents of the outer shelf and upper slope from a decade of shipboard ADCP observations in the Middle Atlantic Bight. J. Geophys. Res. 111, C06003. http://dx.doi.org/10.1029/2005JC003116.

Flather, R.A., 1976. A tidal model of the northwest European continental shelf. Mem. Soc. R. Sci. Liege 10 (No. 6), 141–164.

Greene, C.H., Pershing, A.J., 2003. The flip-side of the North Atlantic Oscillation and modal shifts in slope-water circulation patterns. Limnol. Oceanogr. 48, 319–322.

Halkin, D., Rossby, T., 1985. The structure and transport of the Gulf Stream at 73°W. J. Phys. Oceanogr. 15, 1439–1452.

He, R., Weisberg, R.H., 2002. West Florida shelf circulation and temperature budget for the 1999 spring transition. Cont. Shelf Res. 22, 719–748.

Houghton, R.W., Schlitz, R., Beardsley, R.C., Butman, B., Chamberlin, J.L., 1982. The Middle Atlantic Bight cold pool: evolution of the temperature structure in summer 1979. J. Phys. Oceanogr. 12, 1019–1029.

Joyce, Terrence M., 1991. Review of U.S. contributions to warm-core rings, Reviews of Geophysics, Supplement (U.S. National Report to International Union of Geodesy and Geophysics 1987–1990), pp. 610–616.

Knauss, J.A., 1969. A note on the transport of the Gulf Stream. Deep Sea Res. 16 (Suppl), S117–S123.

Lentz, S.J., 2008a. Observation and a model of the mean circulation over the Middle Atlantic Bight Continental Shelf. J. Phys. Oceanogr. 38, 1203–1221.

Lentz, S.J., 2008b. Seasonal variability in the circulation over the Middle Atlantic Bight Continental Shelf. J. Phys. Oceanogr. 38, 1486–1500.
Linder, C.A., Gawarkiewicz, G.G., 1998. A climatology of the shelfbreak front in the Middle Atlantic Bight. J. Geophys. Res. 103, 18405–18423.
Linder, C.A., Gawarkiewicz, G.G., Taylor, M., 2006. Climatological estimation of environmental uncertainty over the middle Atlantic Bight Shelf and Slope. IEEE J. Ocean. Eng. 31, 308–324.
Loder, J.W., Petrie, B., Gawarkiewicz, G.G., 1998. The coastal ocean off northeastern North America: a large-scale view. In: The Sea, vol. 11, The Global Coastal Ocean, R(egi)onal Studies and Syntheses. Robinson, A.R., Brink, K.H. (eds.). John Wiley, New York, pp. 105–133.
Loder, J.W., Hannah, C.G., Petrie, B.D., Gonzalez, E.A., 2003. Hydrographic and transport variability on the Halifax section. J. Geophys. Res. Ocean. 108 (C11), 8003. http://dx.doi.org/10.1029/2001JC001267.
Lozier, M.S., Gawarkiewicz, G.G., 2001. Cross-frontal exchange in the Middle Atlantic Bight as evidenced by surface drifters. J. Phys. Oceanogr. 31, 2498–2510.
Luo, Y., Rothstein, L., Liu, Q., Zhang, S., 2013. Climatic variability of the circulation in the Rhode Island Sound: a modeling study. J. Geophys. Res. Ocean., 118. http://dx.doi.org/10.1002/ jgrc.20285.
Manning, J., 1991. Middle Atlantic Bight salinity: interannual variability. Cont. Shelf Res. 11, 123–137.
McCarthy, G., Frejka-Williams, E., Johns, W.E., Baringer, M.O., Meinen, C.S., Bryden, H.L., Rayner, D., Duchez, A., Roberts, C., Cunningham, S.A., 2012. Observed interannual variability of the Atlantic Meridional Overturning Circulation at 26.5°N. Geophys. Res. Lett. 39, L19609. http://dx.doi.org/10.1029/2012GL052933.
Mellor, G.L., Yamada, T., 1982. Development of a turbulence closure model for geophysical fluid problems. Rev. Geophys. 20, 851–875.
Mountain, D.G., 2003. Variability in the properties of shelf water in the Middle Atlantic Bight, 1977–1999. J. Geophys. Res. 108 (C1), 3014. http://dx.doi.org/10.1029/2001JC001044.
Osborn, T.J., 2011. Winter 2009/2010 temperatures and a record-breaking North Atlantic Oscillation index. Weather 66, 19–21. http://dx.doi.org/10.1002/wea.660.
Pershing, A.J., Greene, C.H., Hannah, C., Sameoto, D., Head, E., Mountain, D.G., Jossie, J.W., Benfield, M.C., Reid, P.C., Durban, T.G., 2001. Oceanographic responses to climate in the Northwest Atlantic, Oceanography, vol. 14, pp. 76–82.
Rasmussen, L.L., Gawarkiewicz, G., Owens, W.B., Lozier, M.S., 2005. Slope water, Gulf Stream, and seasonal influences on southern Mid-Atlantic Bight circulation during the fall-winter transition. J. Geophys. Res. 110, C02009. http://dx.doi.org/10.1029/2004JC002311.
Ramp, S.R., Beardsley, R.C., Legeckis, R., 1983. An observation of frontal wave development on a shelf-slope/warm core ring front near the shelfbreak south of New England. J. Phys. Oceanogr. 13, 907–912.
Rossby, T., Benway, R.L., 2000. Slow variations in mean path of the Gulf Stream east of Cape Hatteras. Geophys. Res. Lett. 27, 117–120.
Shchepetkin, A.F., McWilliams, J.C., 2005. The Regional Oceanic Modeling System (ROMS): a split-explicit, free surface, topography-following-coordinate oceanic model. Ocean Modell. 9, 347–404.
Shearman, R.K., Lentz, S.J., 2003. Dynamics of mean and subtidal flow on the New England shelf. J. Geophys. *Res.*. 108 (C8), 3281. http://dx.doi.org/10.1029/2002JC001417.
Smeed, D.A., McCarthy, G.D., Cunningham, S.A., Frajka-Williams, E., Rayner, D., Johns, W.E., Meinen, C.S., Baringer, M.O., Moat, B.I., Duchez, A., Bryden, H.L., 2014. Observed decline of the Atlantic meridional overturning circulation 2004–2012. Ocean Sci. 10, 29–38. http://dx.doi.org/10.5194/os-10-29-2014.
Smethie, W.M., Schlosser Jr., P., Bönisch, G., Hopkins, T.S., 2000. Renewal and circulation of intermediate waters in the Canadian Basin observed on the SCICEX 96 cruise. J. Geophys. Res. 105, 1105–1121. http://dx.doi.org/10.1029/1999JC900233.
Taylor, A.H., 2011. The Dance of Air and Sea: How Oceans, Weather and Life Link Together. Oxford University Press, United Kingdom.
Ullman, D.S., Codiga, D.L., 2004. Seasonal variation of a coastal jet in the Long Island Sound outflow region based on HF radar and Doppler current observations. J. Geophys. Res. 109, C07S06. http://dx.doi.org/10.1029/2002JC001660.
Walsh, J.J., Biscaye, P.E., Csanady, G.T., 1988. The 1983-84 shelf edge exchange processes (SEEP)-I experiment: hypotheses and highlights. Cont. Shelf Res. 8, 435–456.
Xu, F.-H., Oey, L.-Y., 2011. The origin of along-shelf pressure gradient in the Middle Atlantic Bight. J. Phys. Oceanogr. 41 (9). http://dx.doi.org/10.1175/2011JPO4589.1.
Zhang, W.G., Wilkin, J.L., Chant, R.J., 2009. Modeling the pathways and mean dynamics of river plume dispersal in the New York Bight. J. Phys. Oceanogr. 39, 1167–1183.
Zhang, W.G., Gawarkiewicz, G.G., McGillicuddy, D.J., Wilkin, J.L., 2011. Climatological mean circulation at the New England shelf break. J. Phys. Oceanogr. 41, 1874–1893.